Nanoelectrónica bidimensional

Saúl Sánchez González

Master's Thesis

Facultad de Ciencias
Universidad de Oviedo

Contents

List of Figures

List of Tables

Agradecimientos

Me gustaría agradecer profundamente a todos los profesores que a lo largo del grado y el máster han dedicado su tiempo a enseñarme y a contagiarme su pasión por la física. También dar las gracias a mis compañeros a lo largo de estos años, su apoyo y motivación han sido muy importantes para mí. Evidentemente no puedo dejar sin mencionar a toda mi familia y mis amigos que me han ofrecido su ayuda siempre que la he necesitado sin pedir nada a cambio. Para acabar no puedo olvidarme de los que fuesen mis tutores a lo largo de este trabajo, Jaime y Amador, gracias por todas las horas dedicadas a este proyecto, por la enorme paciencia para enseñarme un campo que era totalmente nuevo para mí y por las palabras de ánimo en los peores momentos del desarrollo de este.

Introduction

At the annual American Physical Society meeting at Caltech on December 1959, Richard Feynman, one of the greatest minds of all times said " There's plenty of room at the bottom". He considered the direct manipulation of individual atoms as the future of physics and specially of condensed matter physics. This sentence became more and more present in the 1960s when the development of more powerful and precise technology was driven in part by the miniaturization of transistors. About this time, Gordon Moore, co-founder of Fairchild Semiconductor and Intel, stated that the number of components per Integrated Circuit would double every two years for the next decade. This prediction is nowadays known as Moore's Law (Figure 1) and it has proved accurate over several decades. In 2001, the first nanometric transistor was built (130 nm). It was nearly 80 times smaller than its homologue in 1971. With such a small scale, more technical challenges appeared. Overcoming them not only requires a lot of time and research, but also money and investments. And as such, Moore's Law is actually slowing down and it could eventually stop in the near future (e.g. it took Intel about two and a half years to go from a 22 nm processor in 2012 to 14 nm in 2014 and three years to go from there to 10 nm in 2017). Nowadays different and complex approaches are done to make even smaller processors. In 2012 a single atom transistor was achieved using one phosphor atom attached to a silicon surface [1]. This discovery has created an urgent need for a more precise understanding of matter at the nanoscale where quantum effects are becoming more and more important (e.g. Kondo effect, quantum interference...) from the experimental but also from the theoretical point of view. The development of computational tools capable of predicting quantum transport properties of systems at this scale is an increasingly active field of research [2,3].

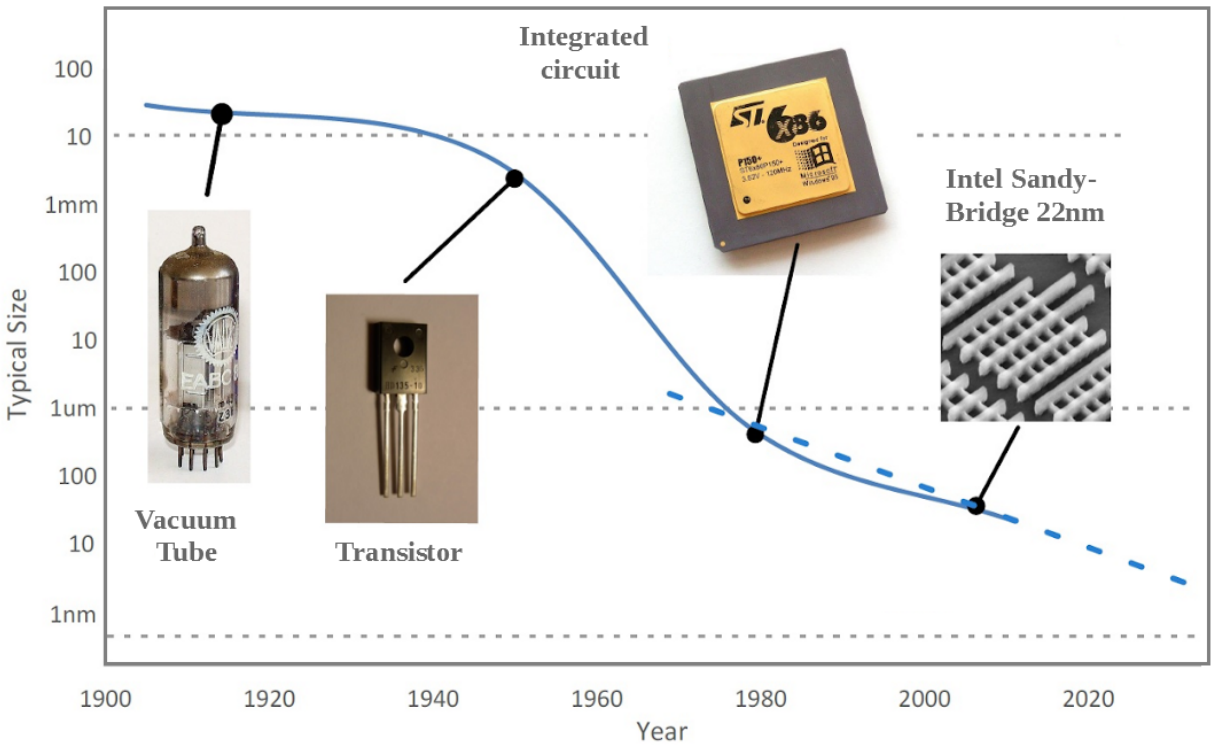

Figure 1: Evolution of the size of a processor with time. Moore's Law is shown as a dashed line whereas the full line represents the experimental achievements through the years.

Molecular junctions in which one or several molecules are connected to metallic electrodes represent a proving ground for our understanding of charge transport and energy level alignment in metal-molecule interfaces at the nanoscale. Most of our current understanding of this alignment builds on effective single-particle descriptions such as the Kohn-Sham (KS) density-functional theory (DFT) [4]. In their description, the energy levels of a molecule close to a surface are determined by Coulomb interactions. Unfortunately, the KS description of excited energy levels is known to be inaccurate, especially for nanometric systems [4]. Apart from that, we also know that when we place our molecule between two metal contacts, screening effects which are not accounted by such methods appear. These are induced by changes in the charged state of the molecule which are not captured by available single-particle descriptions. Two extensions of KS DFT are of special interest nowadays. One is the so called GW approach [7] which is more precise on handling Coulomb interactions and screening effects for the energies of the single-

particle excited states but is very computationally demanding and therefore only allows to study very small molecules. The other one is the DFT+Σ approach which is less demanding and allows the study of larger molecules on a simpler but more limited way (it is already implemented in our simulation tool GOLLUM) [2, 5]. However as I will show, the screening correction implementation was done using a excessively simple model that could not capture all the physics behind the simulations [5]; it only depends on an effective distance that has not a clear physical criteria to be selected. The results we get have therefore some arbitrariness . In fact, when this distance is chosen to match the values obtained from an experiment, the results obtained are not correct. On the other hand, the screening correction explained in this thesis only depends of physical parameters such as the position of the atoms we introduce in the simulation and their Mulliken population [4, 6, 7]; this makes it more complete and also removes the problem of the arbitrariness explained before. The pillar and motivation of this work is then to understand the factors that make the new correction better than the previous one and also to implement it in GOLLUM, making it a much more complete and precise simulation tool that can be used in the future for a wide variety of problems.

The outline of this work can be summarized as follows. In part I we explain the basic concepts of DFT needed to understand this thesis, its limitations to predict the Highest Ocuppied Molecular Orbital (HOMO) and the Lowest Unoccupied Molecular Orbital (LUMO) and so the conductance through the molecule and the most important corrections that have been done to solve them. In part II we focus our attention in the screening effect correction, we review some simple examples and at the end we explain the previous implementation of this correction in GOLLUM. Last but not least, in part III my contributions to this work are highlighted, the new screening correction is explained and implemented in GOLLUM. An example is shown with a Benzenedithiolate (BDT) molecule between Au contacts to find to which extent it is precise. To conclude this thesis I explain

how we will try to generalize this correction in the future when we apply a voltage to the contacts. In the appendix the calculation of Mulliken population is explained.

Part I

Theoretical background

1 Landauer theory of electronic transport

The molecular junctions based on short molecules are examples of systems where transport properties are dominated by elastic scattering events; conduction electrons preserve their quantum mechanical coherence along the junction. These systems are described theoretically within the Landauer formalism [14]. The fundamental idea of this approach is that electron transport through the junction can be modeled as a scattering problem. We assume that the electrodes are ideal reservoirs of electrons at a well defined temperature while the central region is the scattering center (Figure 2).

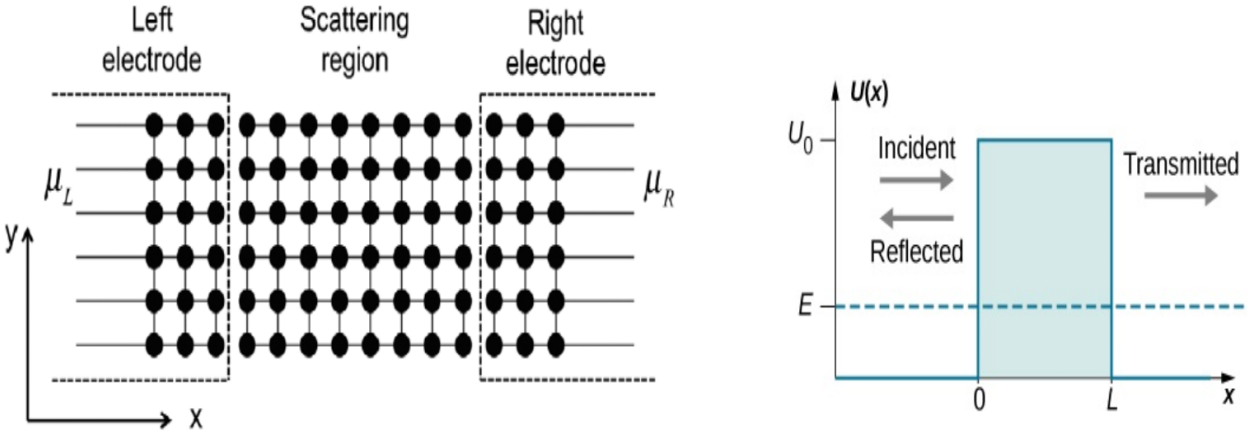

Figure 2: (Left) Scheme of the Landauer scattering problem where a central scattering region is connected to a left and right electrode that act as ideal reservoirs of electrons at a well defined chemical potential μ_L and μ_R. (Right) Analogy with the potential barrier problem in quantum physics.

As a result, all the transport properties of these systems are completely determined by the transmission function $\tau(E, V)$ which describes the probability of electrons to cross the junctions at a given energy E when a voltage V is applied across the system. In general this transmission function depends on V on a non trivial way but for a lot of cases we can make the approximation $\tau(E, V) \sim \tau(E, 0)$. Our molecules are then connected to a left and right (L and R respectively) semi-infinite electrode, each of them with a chemical potential $\mu_{L,R}$ and temperature $T_{L,R}$. The transmission function can be obtained as [10]:

$$\tau(E) = Tr[G^r(E)\Gamma_L(E)G^a(E)\Gamma_R(E)] \tag{1}$$

where $G^{a,r}(E)$ is the advanced (retarded) Green's function and $\Gamma_{L,R}$ describes the broadening of the energy levels of the molecule due to the coupling to the left and right electrodes expressed in terms of the electrode self-energies $\Sigma_{L,R}$ (E) [10].

$$\Gamma_{L,R}(E) = i\left(\Sigma^r_{L,R}(E) - \Sigma^a_{L,R}(E)\right) \tag{2}$$

where $\Sigma^{a,r}(E)$ is the advanced (retarded) electrode self-enery. The charge current has then the form:

$$I(V) = \frac{2e}{h}\int_{-\infty}^{\infty} dE\,\tau(E)\,\left(f_S(E,\mu_S) - f_D(E,\mu_D)\right) \tag{3}$$

where $f_{S,D}$ are the Fermi functions of the source and the drain and $\mu_{S,D}$ are the corresponding chemical potentials such that $\mu_S - \mu_D = eV$. The prefactor 2 is due to the spin degeneracy. To obtain a physical picture we consider an electron with an energy E which is transmitted elastically through the junction region from the source to the drain. After reaching the drain, the electron undergoes inelastic processes (via electron–phonon interactions) and it decays to the chemical potential of the drain. In these processes, the electron releases an energy $E - \mu_D$ in the drain. On the source side, the original electron leaves behind a hole that is filled up by the same type of inelastic processes. In this way,

an energy $\mu_S - E$ is dissipated in the source. The transmission function accounts for the finite probability of an electron to tunnel through the junction, and the Fermi functions account for the occupation probabilities of the initial and final states in the tunneling events. In particular, the appearance of the difference of the Fermi functions is a result of the net balance between tunneling processes transferring electrons from the source to the drain and from the drain to the source (Figure 3).

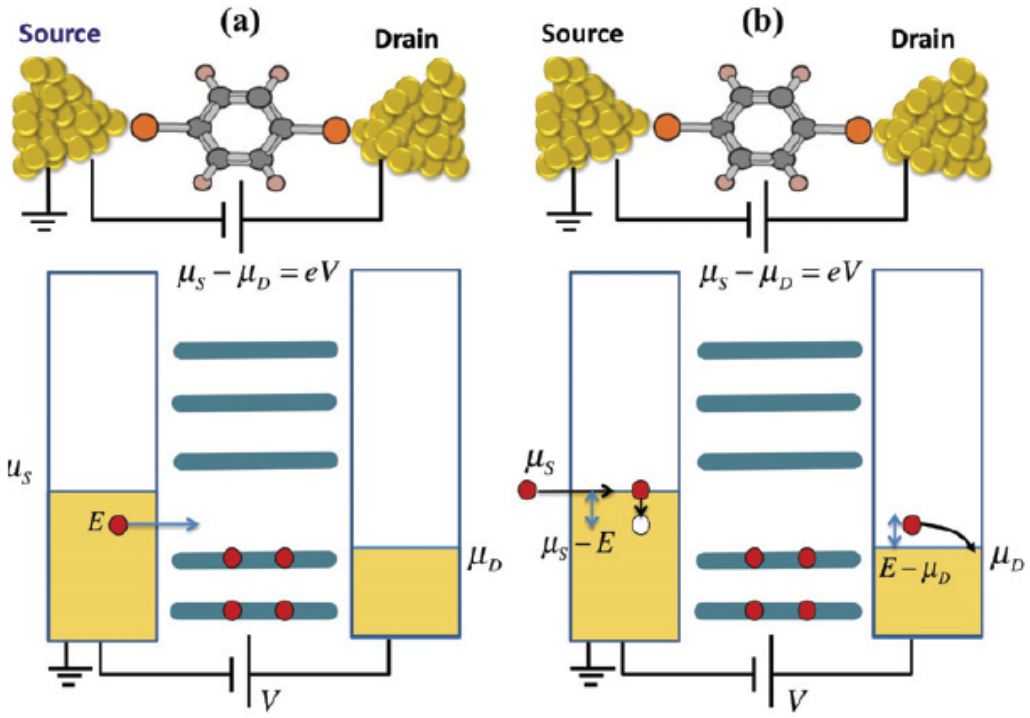

Figure 3: (a) The source and drain are described by Fermi seas with electrons occupying states up to the HOMO. If a voltage V is applied across the junction $\mu_S - \mu_D$ = eV. (b) When an electron of energy E tunnels from the source to the drain, it leaves a hole behind. The electron releases its excess energy E $-\mu_D$ in the drain, while the hole is filled up dissipating an energy equal to μ_S- E in the source.[6]

To relate this concepts to a physical quantity that can be measured in the experiments we define the differential conductance G as:

$$G = \frac{dI}{dV} = \frac{2e^2}{h}\frac{d}{dV}\int_{-\infty}^{\infty} \tau(E)\,\left(f_S(E,\mu_S) - f_D(E,\mu_D)\right)dE \tag{4}$$

Using the low temperature expansion we get to:

$$G = \frac{2e^2}{h}\,\tau(0,0) = G_0\,\tau_0 \tag{5}$$

where τ_0 is the zero-bias transmission function at the Fermi energy (we use it as the origin). The calculation of the electrode and molecule self-energies and thus the conductance through the junction is usually based in density functional theory (DFT) [6]. We now explain the fundamental concepts of it to understand this thesis.

2 Fundamentals of DFT

The dynamics of a time-independent non-relativistic system of N electrons are governed by the Schrödinger equation:

$$E\Psi = H\Psi \tag{6}$$

where Ψ is the many electron wavefunction, E is the system energy and H is the Hamiltonian of the system given by (in atomic units)

$$H = \sum_{i=1} N\left(-\frac{1}{2}\nabla_i^2 - Z\sum_R \frac{1}{|\mathbf{r_i} - \mathbf{R}|}\right) + \frac{1}{2}\sum_{i\neq j}\frac{1}{|\mathbf{r_i} - \mathbf{r_j}|} \tag{7}$$

Here $\boldsymbol{r_i}$ is the position of electron i, whilst the nuclei are clamped at positions $\boldsymbol{R}$. We are interested in the electron behaviour so we have decoupled the nuclear and electronic degrees of motion within the Born-Oppenheimer approximation and focus just on the electronic ones. The first term is the many-body kinetic energy operator which yields the electronic kinetic energies; the second term represents the interaction of the electrons with the bare nuclei. Electron-electron interactions are described by the final term. Since the many-electron wavefunction contains $3N$ degrees of freedom this makes the problem computationally intractable for a system with more than a few electrons. Further, the

electron-electron Coulomb interaction results in the electronic motions being correlated which makes this problem even more difficult, as the effect of this correlation prevents a separation of the electronic degrees of freedom into N single-body problems. Moreover, the interaction is too strong to be treated as a perturbation so we have to look for approximations that make this problem simpler.

The first historical approach to this many body problem was the Hartree-Fock (HF) method but it only incorporated electron-electron interactions via a mean field potential and therefore neglected correlation. A more complete approach is DFT which treats the electron density as the central variable rather than the many-body wavefunction. This conceptual difference leads to a remarkable reduction in difficulty: the density is a function of three variables, i.e. the three Cartesian coordinates, rather than $3N$ variables as the full many-body wavefunction is. DFT is based upon the following Hohenberg-Kohn theorems [16]:

Theorem 1 *The external potential is a unique functional of the electron density only. Thus the Hamiltonian, and hence all ground state properties, are determined solely by the electron density.*

Theorem 2 *The groundstate energy may be obtained variationally: the density that minimises the total energy is the exact groundstate density.*

Although these two theorems prove the existence of a universal functional, they do not give any idea of the nature of it. In fact, if we want to calculate the ground state density we have to minimise this functional that in principle we don't know. In order to do so, we use the Kohn-Sham (KS) formulation. This is based upon a trick whereby we map the fully interacting system of N electrons onto a fictitious auxiliary system of N non-interacting electrons moving within an effective KS potential, V_{KS}, thereby coupling the electrons. The requirement that the minimization of the exact Hamiltonian and the KS Hamiltonian with respect to the electron density gives the same electron density and energy of

the ground state leads to a unique V_{KS} potential for each full Hamiltonian of interacting electrons, so that there is a one to one correspondence between the two. **If we know the exact V_{KS} we can solve the non-interacting Hamiltonian and obtain the properties of the interacting (exact) one on a much simpler way**. We can see schematically:

$$H_{Exact} \longrightarrow H_{KS}[n(\boldsymbol{r})] = T[n(\boldsymbol{r})] + \sum V_{KS}\,[n(\boldsymbol{r})] \tag{8}$$

$$E_{Exact} \longrightarrow E_{KS}\,[n(\boldsymbol{r})]$$

The minima satisfies for the exact KS potential:

$$n_0 = n_{Exact,0} = n_{KS,0} \tag{9}$$

$$E_0 = E_{Exact,0} = E_{KS,0}\;[n_0(\boldsymbol{r})]$$

where $E_{Exact,0}$ and $E_{KS,0}$ denote the exact energy of the ground state of the interacting system and the obtained with KS theory and $n_{Exact,0}$ and $n_{KS,0}$ its electronic density. E_0 and n_0 are the ground state energy and density of the system. Without looking at details we are required to solve the Schrödinger-type equations:

$$\left(-\frac{1}{2}\nabla^2 + V_{KS}\right)\Psi_{K,i}(\boldsymbol{r}) = \epsilon_{KS,i}\,\Psi_{K,i}(\boldsymbol{r}) \tag{10}$$

where Ψ are the eigenstates (orbitals) of equation 10 whereas ϵ correspond to the eigenenergies. From now and on we will call them KS eigenstates and eigenenergies. The charge density $n(\mathbf{r})$ is constructed from the Kohn-Sham orbitals as:

$$n(\boldsymbol{r}) = \sum_{i=1}^{N} \Psi^*_{K,i}(\boldsymbol{r})\Psi_{K,i}(\boldsymbol{r}) \tag{11}$$

The KS formulation thus succeeds in transforming the N-body problem into N single-body identical Hamiltonians, with the same KS potential. Formally there is no physical interpretation of these $\epsilon_{KS,i}$ and KS orbitals: they are merely mathematical artefacts that facilitate the determination of the true ground state density. On the other hand, the total energy (E) has a physical interpretation and can be calculated as:

$$E = \sum_{i=1}^{N} \epsilon_{KS,i} - E_H[n_0] + E_{KS}[n_0] - \int V_{KS}(\boldsymbol{r})\, n_0(\boldsymbol{r}) d\boldsymbol{r} \tag{12}$$

where $E_H[n_0]$ and $E_{KS}[n_0]$ denote the Hartree and the KS energy of the ground state. The last three terms of this expression account for the double counting of the electron-electron interaction. Unfortunately, in this formulation it is almost impossible to know the KS exact potential and then some approximations are done. This produces some problems that become very important when we are working with nanoelectronics. On next section we review them briefly.

3 KS theory limitations in nanoelectronics

It is extremely important for this manuscript to note that there is not a formal physical interpretation of these single-particle Kohn-Sham eigenvalues and orbitals. The exception is the highest occupied state, for which it can be shown that **the eigenvalue corresponding to the highest occupied state yields the ionisation energy of the system only for the exact KS potential (Janak's theorem)** [17]. Unfortunately, to know this exact potential is almost impossible and thus we introduce approximate functionals based upon the electron density to describe this term. Probably the most popular that is implemented in all the DFT computational codes is the generalized gradient approximation (GGA). Within this approximation the HOMO and LUMO are not correctly calculated because GGA does not estimate right the Coulomb interactions among electrons. **There are two**

aspects to this defficiency (1) Coulomb interaction among electrons of an isolated system (remember that GGA is not the exact KS potential and thus Janak's theory doesn't hold) (2) This Coulomb interaction is not the same if the system is isolated or near a metallic surface that screens it. The fix of the first one is called gas phase correction because it assumes that the system is isolated meaning in the gas phase. As a summary we have two very important and fundamental problems:

$\rightarrow$ GGA is not the exact KS potential of an isolated system and so the position of the HOMO and LUMO with respect to the Fermi energy (E_F) ,which we will use as the origin for this manuscript, is not correctly calculated

$\rightarrow$ GGA does not take into account screening effect if the system is not isolated but near a metallic surface.

So the position of the HOMO and the LUMO is not correctly calculated because of these two reasons. This implies that GGA, as all the computationally feasible approximations, gives a wrong results for the conductance as I will explain later. This represents a huge problem for nanoelectronics because of two reasons. (1) The KS energies are widely used to study solids because they are easy to calculate and in general predict the correct band structure of a material. This description is no longer valid for nanostructures or strongly correlated systems and so a different approach is needed [6]. (2) The HOMO-LUMO gap overestimation mentioned above leads to a KS conductance that differs a lot from the exact one. On (Figure 4) a schematic graph is displayed where the KS transmission function is compared with the exact one.

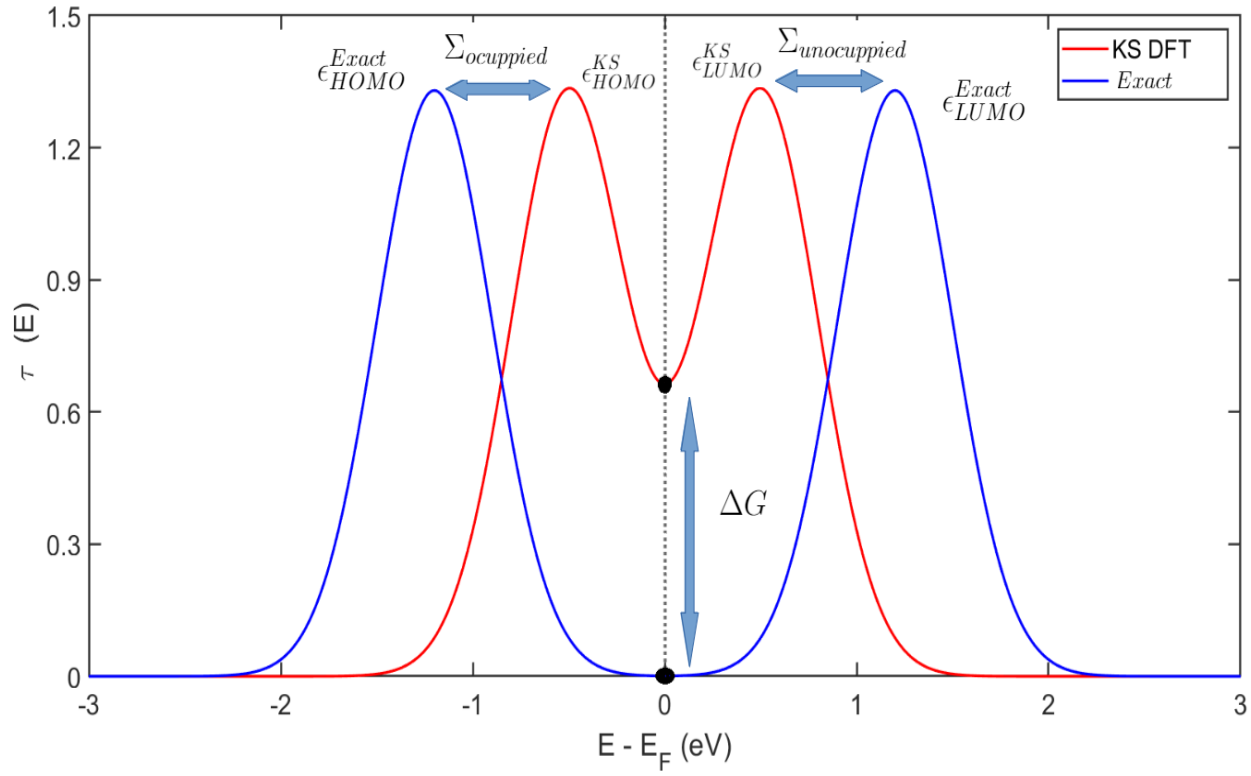

Figure 4: Scheme of the transmission function for KS DFT (red) and the exact tranmission (blue) where ϵ^{KS}_{HOMO}, ϵ^{KS}_{LUMO} ϵ^{Exact}_{HOMO} and ϵ^{Exact}_{LUMO} denote the position of the HOMO and LUMO for KS and the exact result. $\Sigma_{ocuppied}$ and $\Sigma_{unocuppied}$ denote the HOMO-LUMO miscalculation done with KS DFT while ΔG the error in the conductance.

As explained before, the position of the HOMO and LUMO predicted with the KS formalism does not match the exact solution. **The difference among them is the correction we want to introduce** ($\Sigma_{ocuppied}$ for the HOMO and $\Sigma_{unocuppied}$ for the LUMO). The error in conductance (ΔG) is also shown.

A difference in one order of magnitude between the KS and the exact conductance is common. Of course this is a huge problem that limits us when we study a lot of complex systems at the nanoscale. To predict the position of the HOMO and the LUMO and so the transmission and conductance through the molecule in a precise way, we have to correct DFT-GGA self interaction errors and screening effects. To do so, two different approaches are commonly used, the GW and the DFT+Σ correction.

4 GW correction

This method is based in many body perturbation theory [6]. On it, the retarded Green's function of the molecule is given by:

$$G^r_{GW}(E) = \left[(E + i\eta)\, S - (H_{KS} - V_{KS}) - \Sigma^r_{GW}(E) - \Sigma^r_L(E) - \Sigma^r_R(E)\right]^{-1} \qquad (13)$$

We substract the KS potential V_{KS} from the DFT Hamiltonian H_{KS} and add the GW self-energy Σ_{GW}. As GW self-energy depends on G^r (E) at all energies, the equations for it have to be solved self-consistently for all its values. It drastically improves the description of the electronic structure of metal-molecule interfaces compared to DFT [7] at the cost of being computationally demanding. Two fundamental and technical advantages are clear. (1) GW improves the fictitious potential (V_{KS}) compared to LDA or GGA. This improvement is because GW treats better the naked (nanostructure in vacuum) but also the screened (molecule between contacts) Coulomb interaction thanks to the Σ_{GW} self energy introduction. (2) It searches for the poles of the many body Green's function which correspond to the quasiparticle excitations instead of the eigenenergies (ϵ_{KS}) of the fictitious Hamiltonian which have no physical meaning as explained before. For all these reasons self-consistent GW conductance calculations for simple molecules in idealized junction geometries were shown to be in good agreement with experiments [7,8]. It is then interesting to find another numerically easier method that allows the study of large molecules. Such method is the non-self consistent correction DFT+Σ. This latter approach has shown to predict conductance in good agreement with single-molecule experiments [6,7,8] and also with the GW correction for some molecules [10]. However, its formal justification is limited to weakly coupled molecules. Specifically, charge transfer screening as well as inelastic scattering are not accounted by such methods.

5 DFT+Σ correction

As explained in the previous section, only the KS eigenvalue corresponding to the HOMO can be obtained on a precise way because it corresponds to the ionisation energy of the system for the exact KS potential (Janak's theorem). Therefore we can correct the KS HOMO (ϵ_{HOMO}) and LUMO (ϵ_{LUMO}) energies by calculating the ionization potential (IP) and the electron affinity (EA) from total energy calculations:

$$EA = E(N-1) - E(N) \qquad IP = E(N) - E(N+1) \tag{14}$$

where $E(N)$ is the total energy of the system with N electrons. We have to take into account that the total energy of the system (that we obtain with a DFT code) is not the sum of the KS eigenenergies . EA is the energy gained by adding an electron to a system and IP is the energy required to remove one electron entirely from a system. With it we can get the shift we need to apply to ϵ_{HOMO} and ϵ_{LUMO} to obtain their correct values **for the molecule in vacuum**:

$$\Delta_{unoccupied} = -(\epsilon_{LUMO} + EA) \qquad \Delta_{ocuppied} = -(\epsilon_{HOMO} + IP) \tag{15}$$

where $\Delta_{unoccupied}$ and $\Delta_{occupied}$ represent the shift in the LUMO and HOMO. This first correction is called **gas phase correction**. We can see then that the corrected HOMO is now at -IP as it should (we have to be careful with the signs we choose) and the LUMO is at -EA.

To clarify the validity of this approximation we use the Hubbard dimer as an example [15]:

$$H = -t \sum_{\sigma} \left(c_{1\sigma}^{+} \, c_{2\sigma} + h.c \right) + U \sum_{i} n_{i\uparrow} \, n_{i\downarrow} + \sum_{i} v_i \, n_i \tag{16}$$

where v are the on site energies, t the hopping terms, U the Coulomb energies, c_i^{+} are the creation while c_i the anhilitation operators on the i-th site and $n_{i\uparrow}$ and $n_{i\downarrow}$ are the spin up and down density operators. $\Delta v = v_2 - v_1$ represents the difference in on-site potential between both atoms. It is useful to have a very simple physical scheme in mind (Figure 5).

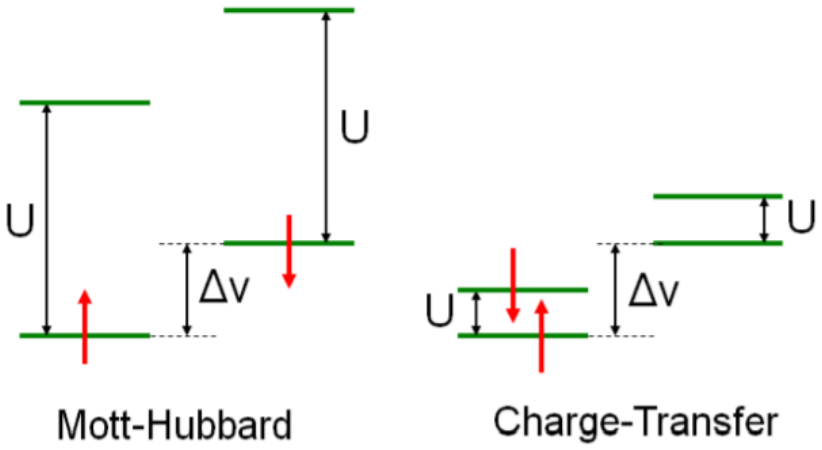

Figure 5: Energetic configuration of the Hubbard dimer. (Left) Charging energy is greater than the difference in on-site potentials (Right) Charging energy is smaller than the difference in on-site potentials [15]

We are not going to explain the differences between the Mott-Hubbard and the charge-transfer regime but it is interesting to see how correlations affect the precision of our calculations. As the Hubbard Hamiltonian is possibly the simplest model of a interacting electron system, it allows us to solve it analytically and see the differences with KS DFT (e.g. in semiconductors with small gaps, such as germanium, approximate Kohn-Sham (KS) gaps are often zero, making the material a band metal, but an insulator in reality). We analyze two cases (1) $U = 1$ and $2t = 1$,weakly correlated system (2) $U = 5$ and $2t = 1$,

strongly correlated system. (Figure 6).

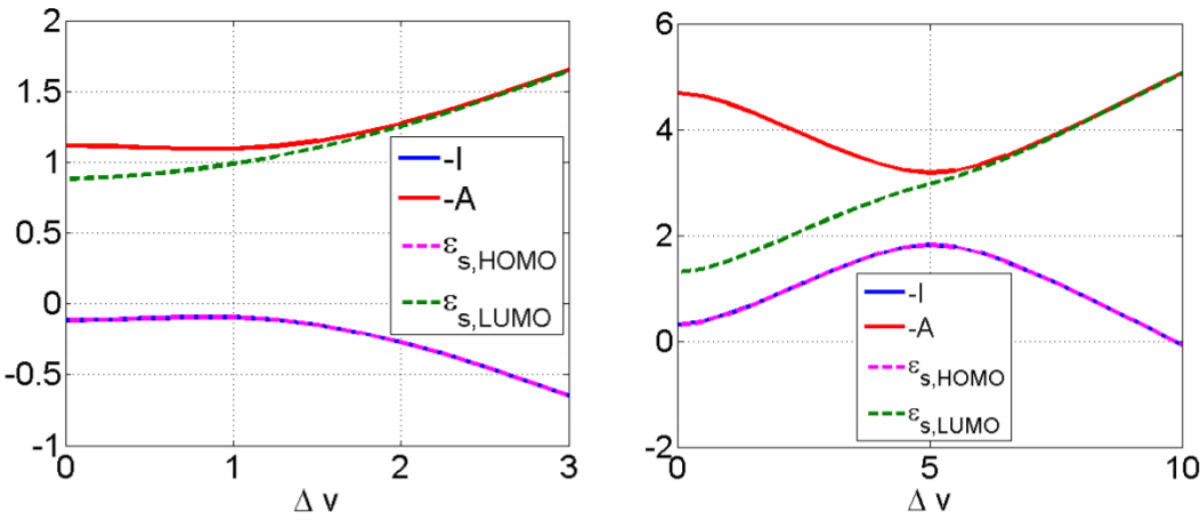

Figure 6: (Left) Plot of -A, -I, ϵ_{HOMO} and ϵ_{LUMO} with $U = 1$ and $2t = 1$ (Right) Plot of -A, -I, ϵ_{HOMO} and ϵ_{LUMO} with $U = 5$ and $2t = 1$. We denote A as the electron affinity in the figure and I as the ionization potential (instead of EA and IP in the equations)[15]

The KS HOMO (ϵ_{HOMO}) is always at -IP but the KS LUMO (ϵ_{LUMO}) is not at -EA (it becomes clear that for a stronger correlation the approximation of the LUMO by EA is no longer valid). To understand the difference between KS and the exact solution better, we show their spectral functions. We represent their δ-function poles with lines whose height is proportional to the weights via a simple sum-rule (Figure 7). On the figure E_g is the real gap of the system which can be used to decide if they are metals (E_g=0) or insulators (E_g>0) and $E_{g,s}$ is the KS gap:

$$E_g = IP - EA \qquad E_{g,s} = \epsilon_{LUMO} - \epsilon_{HOMO} \tag{17}$$

As we have explained both of them are different and in fact the stronger the correlations, the more different they become. To quantify this difference we define:

$$\Delta_{xc} = E_g - E_{g,s} \tag{18}$$

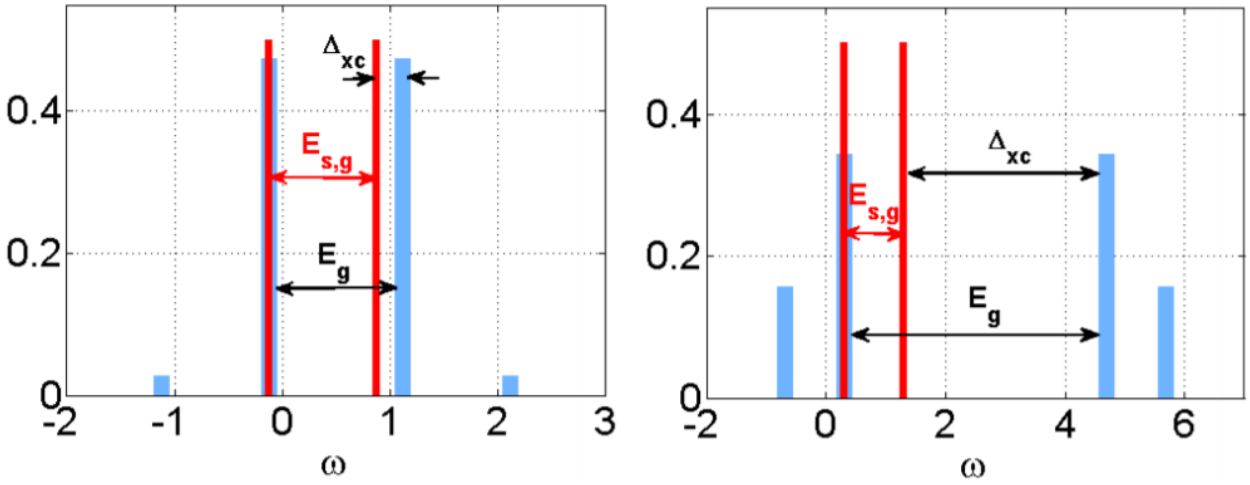

Figure 7: (Left) Spectral function of symmetric dimer for $U = 1$, and $2t = 1$. We denote A as the electron affinity in the figure and I as the ionization potential (instead of EA and IP in the equations). The physical exact peaks are plotted in blue, the KS in red. Here $IP = 0.1$, $EA = -1.1$ and $\epsilon_{LUMO} = 0.9$ (Right) Same as left but now $U = 5$. Here $IP = -0.3$, $EA = -4.7$, and $\epsilon_{LUMO} = 1.3$ [15]

On (Figure 7 Left) we plot the spectral functions for the symmetric case, for $U = 1$, when $2t = 1$. The gap is the distance between the highest negative pole (at IP) and the lowest positive pole (at -EA). We see that the exact spectral function also has peaks that correspond to higher and lower quasi-particle excitations. If we now compare this to the exact KS Green's function G_S, we see that, by construction, G_S always has a peak at -IP, whose weight need not match that of the exact function. It has only two peaks, the other being at ϵ_{LUMO}, which does not coincide with the position of the exact peak. This is so because the KS scheme is defined to reproduce the ground-state occupations, nothing else. **For a weakly correlated system, the KS spectral function can be a rough guide to the true quasiparticle spectrum**. On the other hand, when the correlation is very strong (Figure 7 Right), the KS spectral function is not even close to the exact spectral function. Now the two lowest-lying exact peaks approach each other, as do the two highest lying peaks, therefore increasing the quasi-particle gap and thus giving a wrong result for the conductance through the molecule as explained on section 3.

Apart from that, we have to take into account that **the EA and IP are not the same for the isolated molecule (this is how we have done the gas phase correction) that for the molecule placed in the junction where screening effects become present**. To compute the IP and EA of the molecule directly on a nanostructure in a junction is not feasible because of various reasons (1) It is computationally very demanding (2) If you add an electron to the nanostructure, a fraction of the electron will not remain in the molecule, but will spread to the electrodes. A protocol for a nanostructure in a junction is then: (1) Compute EA and IP of an isolated molecule (e.g. in the gas phase, we have already done it). We can see that with GGA, $E(N+1) - E(N)$ and $E(N) - E(N-1)$ estimate better the HOMO and LUMO correct position that $\epsilon_{HOMO,LUMO}$. Because of that, we can use GGA to make a good estimation of IP and EA for the nanostructure in vacuum. With it we solve the HOMO-LUMO gap miscalculation partially but another correction due to the screening of the electrodes is needed. (2) Correct IP and EA for the presence of the electrodes (e.g. screening correction). This will be done using the known "image charge method" that we learnt in our Electromagnetism undergraduate course. Because of that sometimes we will call the screening correction the image charge correction.

Part II

Screening effect correction

Apart from the gas phase correction we know that when a molecule is close to a metallic surface, screening interactions (electrons of the molecule "see" the electrons in the contacts) will change the energy levels , shifting the occupied levels up and the unoccupied levels down (Figure 8) [7]. Before explaining the image charge method in depth, it is interesting to investigate to what extent the GW results can be described by a classical image charge model.

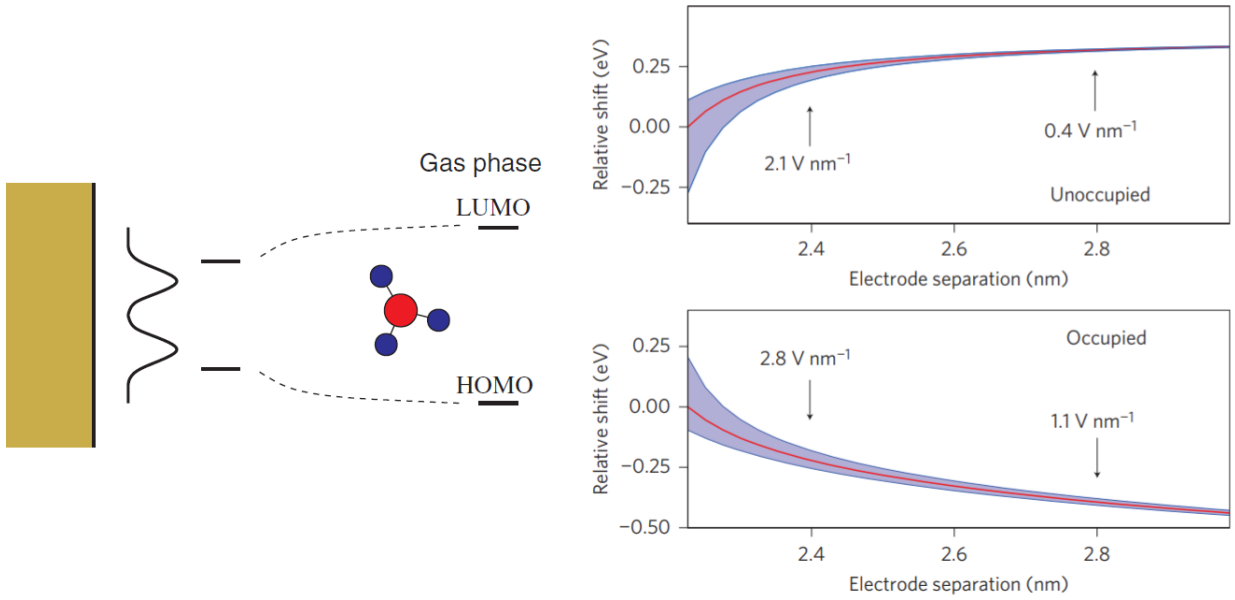

Figure 8: (Left) Reduction in a molecule's energy gap when it approaches a polarizable surface [4] (Right) Level shifts predicted by the image-charge model with uncertainties for 5,15-di(p-thiolphenyl)-10,20-di(p-tolyl)porphyrin (ZnTPPdT) coupled to gold (example) [11] .

The electrostatic energy of a point charge q located in vacuum at (0, 0, z) above a polarizable medium $z < z_o$ is given by (a.u):

$$V = \frac{qq'}{4\,(z - z_o)} \tag{19}$$

The image charge is q'=q (1-ϵ) (1+ϵ) where ϵ is the dielectric constant of the medium [4]. Khom showed that the energy of a classical point charge above a quantum jellium surface follows this equation with $q' = -q$ ($\epsilon = \infty$, perfect metal) with the image plane z_o lying 0.5-0.9 Å outside the surface depending on the electron density [4]. On (Figure 8 Right) we show an example of the HOMO-LUMO shift when we approach a ZnTPPdT molecule to a metallic surface. Ab initio GW calculations have found the same asymptotic form of the potential felt by an electron outside a metallic surface [4]. We show on (Figure 9) the GW energy gap of benzene on NaCl, TiO_2, and Ti surfaces and compare it to the classical image charge model.

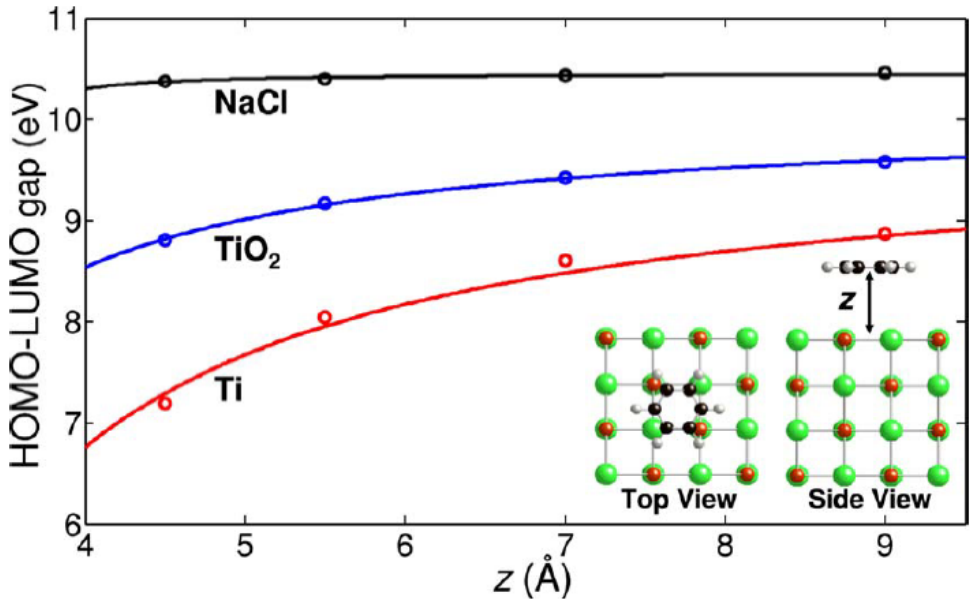

Figure 9: GW energy gap of benzene on NaCl, TiO_2, and Ti surfaces (circles) as a function of the distance to the surface, and the best fit to the classical model (full lines) [4]

It seems reasonable to conclude that the asymptotic position of the electronic levels of a molecule outside a surface would also follow the image potential of the equation (unoccupied and occupied levels experience a shift in opposite directions). Now that we have understood why this method is a good approach to the problem of the HOMO-LUMO gap miscalculation (without being so computationally demanding as the GW approximation) we explain the image charge method.

1 Image Charge Method

A lot of problems in electromagnetism involve boundary surfaces on which the potential or the charge density is known. Unfortunately, solving the Poisson equation for these cases can be very difficult. However, in some particular configurations, the equipotential surfaces of the conductors are reproduced by replacing them by some image charges inside them. The validity of this method rests upon a corollary of the uniqueness theorem which states that the electric potential in a given volume is uniquely determined if both, the charge density throughout the region and the value of the electric potential on all boundaries are known. As the boundary is the metal surface, our result will be valid outside the electrodes. With this technique, usually called image charges method [12,13] the solution can be written as the sum of well known potentials of point charges. We present the easiest example of this method, a point charge in front of a grounded conducting plane.

2 Charge in front of a grounded conductor

We have to make sure that all the boundary conditions are satisfied; as the plane is grounded, the potential at all its points is $V = 0$ (Figure 10).

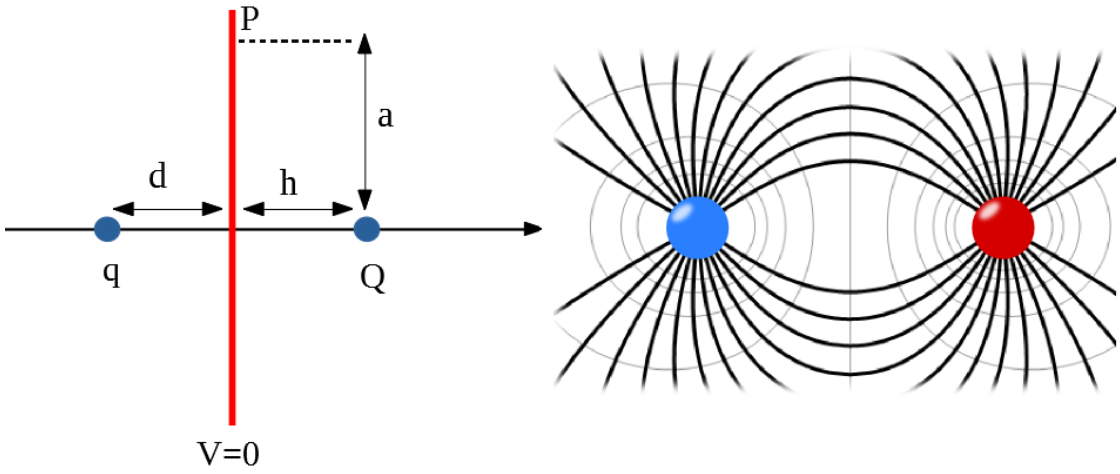

Figure 10: (Left) Scheme of the problem where P is an arbitrary point in which we impose the boundary conditions and the red line is the conductor surface. The black line represents the z=0 plane. (Right) Equipotential lines (grey) and electric field lines (black) of the problem.

The potential at the middle point between both charges and then at point P (Figure 10) is then:

$$V_O = \left(\frac{q}{d} + \frac{Q}{h}\right) = 0 \qquad V_P = \left(\frac{q}{\sqrt{d^2 + a^2}} + \frac{Q}{\sqrt{h^2 + a^2}}\right) = 0 \tag{20}$$

Solving these equations we obtain $Q = -q$ and $d = h$. This is actually the expected result because of the symmetry of the problem. With the boundary conditions satisfied, we calculate the potential at an arbitrary point (x, y, z) above the plane $z = 0$ (red line in Figure 10), taking into account the position of the charges is $q\,(0, 0, d)$ and $-q\,(0, 0, -d)$.

$$V = q\left[\frac{1}{\sqrt{x^2 + y^2 + (z - d)^2}} - \frac{1}{\sqrt{x^2 + y^2 + (z + d)^2}}\right] \tag{21}$$

As we saw on (Figure 3) we need two planes to represent the contacts to which our molecule is connected. On part III we will see what happens when we apply a voltage V to the plane.

3 Charge between two grounded planes

When we place the image charge of q to the right part of the right plane we make the potential at all its points zero but we change the potential in the left one (it is not zero anymore). This can be solved by putting a new image charge that compensates the effect of the previous one, this idea is repeated an infinite number of times. We put an infinite set of image charges to both sides of the planes to cancel their contributions by pairs (Figure 11).

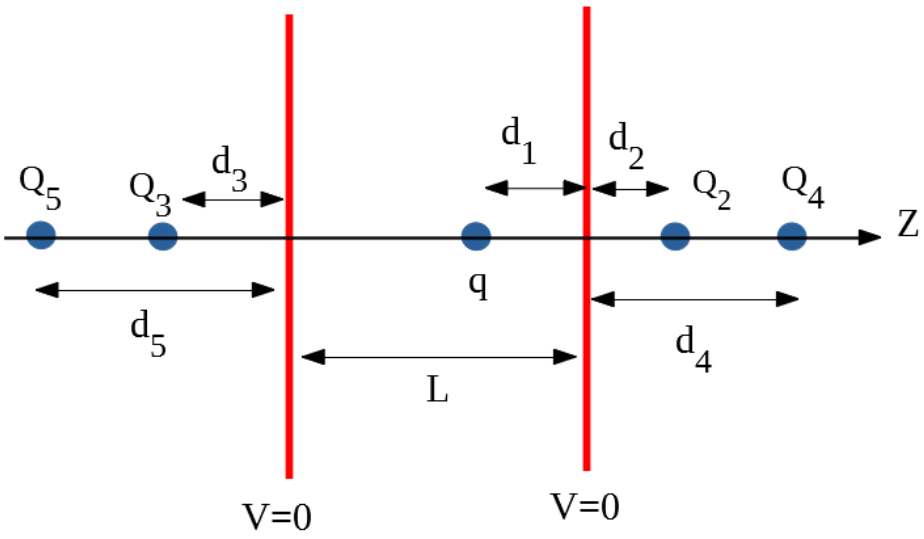

Figure 11: Infinite set of image charges for the point charge between two grounded conducting planes problem

We can get then a recurrence law for the charges and the distances of the form:

$$d_n = L + d_{n-1} \qquad Q_n = -Q_{n-2} \qquad n \text{ even} \tag{22}$$

$$d_n = L + d_{n-3} \qquad Q_n = -Q_{n-2} \qquad n \text{ odd} \tag{23}$$

With the boundary conditions satisfied, we calculate the potential at an arbitrary point P(x,y,z) :

$$V = \frac{q}{\sqrt{r^2+z^2}} + \sum_{neven}^{\infty} \frac{Q_{neven}}{\sqrt{r^2+(z-d_1-d_{neven})^2}} + \sum_{nodd}^{\infty} \frac{Q_{nodd}}{\sqrt{r^2+(z-d_1+L+d_{nodd})^2}} \tag{24}$$

where $r^2 = x^2 + y^2$. This result will be very important for the new screening correction on part III. In future works we will study the effect of applying a different voltage on each plane and how it changes the position of atomic orbitals. Even though it has not yet been implemented in GOLLUM we sum up our analytical results at the end of this thesis.

4 Previous screening correction

To understand the differences and advantages of the new method over the previous one it is interesting to explain the latter very briefly. The previous screening correction used a simple image charge model where the molecule is replaced by a point charge located at the middle point of the molecule and where the image planes are placed at an arbitraty distance a (chosen by the user) above the electrodes surfaces leading to [2,5]:

$$\Delta_{unoccupied} = \frac{e^2}{8\pi\epsilon_0}\frac{ln2}{a} \qquad \Delta_{occupied} = -\Delta_{unoccupied} \tag{25}$$

where a is the distance between the image plane and the point image charge. The total correction $\Sigma_{occupied}$ and $\Sigma_{unoccupied}$ (gas phase+screening) will have then the form:

$$\Sigma_{occupied} = -IP - \epsilon_H + \Delta_{occupied} \qquad \Sigma_{unoccupied} = -EA - \epsilon_L - \Delta_{unoccupied} \tag{26}$$

where ϵ_H and ϵ_L are the KS HOMO and LUMO energies from a DFT calculation. First we apply the gas phase correction so the HOMO is placed at -IP and the LUMO at -EA as explained before (naked Coulomb interaction). After that, the HOMO (LUMO) is shifted down (up) with $\Delta_{occupied}$ ($\Delta_{unoccupied}$) because of the electrodes screening. To explain this result we shall discuss the calculation of the energy of a linear chain of ions of alternate signs (e.g. Na^+ and Cl^-).

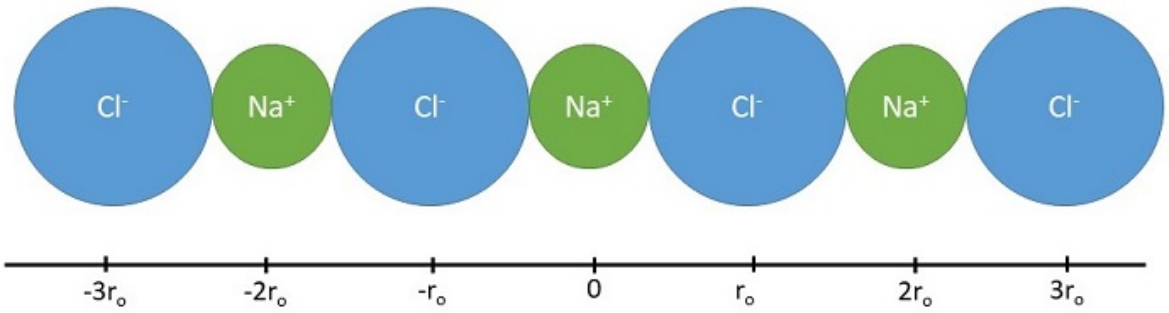

Figure 12: Linear chain of ions of alternate sign

A reference sodium ion has two negative chloride ions as its first neighbors on either side at $\pm r_0$ so the Coulombic interaction is:

$$-\frac{e^2}{4\pi\epsilon_0 r_0} - \frac{e^2}{4\pi\epsilon_0 r_0} = -\frac{2e^2}{4\pi\epsilon_0 r_0} \tag{27}$$

Similarly the repulsive energy due to the next two positive sodium ions at a distance of $2r_0$ is:

$$+\frac{e^2}{4\pi\epsilon_0 (2r_0)} + \frac{e^2}{4\pi\epsilon_0 (2r_0)} = +\frac{2e^2}{4\pi\epsilon_0 (2r_0)} \tag{28}$$

The total energy due to all the ions in the linear array is then:

$$E_{total} = \frac{2e^2}{4\pi\epsilon_0 r_0}\left(1 - \frac{1}{2} + \frac{1}{3} + ...\right) = \frac{2e^2}{4\pi\epsilon_0}\frac{ln2}{r_0} = \frac{2e^2}{4\pi\epsilon_0}\frac{ln2}{r_0} \tag{29}$$

where the factor 4 is due to the chain double counting effects and that $r_0 = 2a$. **The only parameter this previous screening correction takes into account is the distance between the image plane and the point charge image (a) which can be chosen arbitrarily (it does not have a clear physical criteria to be chosen)**. This is very useful when we already know the properties of the molecule we want to analyze so that a might be "adjusted" to deliver the correct results. Unfortunately, it is almost impossible to have an initial guess for a without previous information. One hopes for the best and assumes that the choice of a should be guided by physical intuition, but we shall show here with a well-known example how physical intuition leads to wrong results. As a consequence, no physical intuition can be brought whenever one faces a new phsyical problem or experiment, so the results of the ensuing simulations might be completely wrong. This makes GOLLUM an improvable simulation tool. On the other hand, our correction relies only in the atom positions that are known from the start and their Mulliken population which are physical meaningful quantities. We will show how the new implementation leads to correct estimates for G and so removes all the arbitrariness and sense of loss from the previous implementation. On part III we will compare both models for a Benzeneditholate (BDT) molecule between Au leads.

Part III

My contribution

1 New screening correction

We have been writing about the classical screening correction and atomic orbitals but the connection between both topics may seem loose. To understand it better we repeat the same calculation that for the point charge between two grounded planes but from a quantum mechanical point of view [11]. We start our calculation from the output of SIESTA (Spanish Initiative for Electronic Simulations with Thousands of Atoms) [18], a DFT code that uses localized, non-orthogonal pseudo-atomic wavefunctions as basis set for the electronic wavefunctions. We obtain the Hamiltonian (H) and the overlap matrix (S) describing both molecular and leads atoms from a calculation with the molecule placed in the junction. From these matrices we take the submatrices H_{mol} and S_{mol} spanned only by the basis functions of the atoms in the molecule. The KS eigenenergies ϵ_{KS} and eigenvectors ψ_i for the molecule in the junction are obtained from the equation.

$$H_{mol}\,\psi_i = \epsilon_{KS,i}\,S_{mol}\,\psi_i \tag{30}$$

We approximate the orbital charge distribution at the molecule by a collection of point charges placed at the atom's position R_ν. The charge at each point is approximated by the so-called Mulliken charge $|\psi_{i,\nu,\alpha}|^2$. In the appendix we explain very briefly how to calculate them.

$$\rho_i\,(r) = -e\sum_{\nu}\sum_{\alpha}|\psi_{i,\nu,\alpha}|^2\,\delta(r-R_\nu) \tag{31}$$

where e is the electron charge and $\psi_{i,\nu,\alpha}$ are the coefficients of the i-th eigenstate of the orbital α of atom ν with position R_ν. The image charge energy for a point charge distribution placed between two image planes at $z = 0$ and $z = L$ is then [11]:

$$\Delta_i = \frac{1}{8\pi\epsilon_0}\sum_{\alpha=1}^{N}\sum_{\beta=1}^{N}\rho_i(r_\alpha)\rho_i(r_\beta)\left(\sum_{n=1}^{\infty}\frac{1}{\sqrt{(x_\alpha+x_\beta-2nL)^2+r_{\alpha\beta}^2}}+\right.$$
$$\left.+\frac{1}{\sqrt{(x_\alpha+x_\beta+(n-1)L)^2+r_{\alpha\beta}^2}}-\frac{1}{\sqrt{(x_\alpha-x_\beta+2nL)^2+r_{\alpha\beta}^2}}-\frac{1}{\sqrt{(x_\alpha-x_\beta-2nL)^2+r_{\alpha\beta}^2}}\right) \tag{32}$$

where x_α is the x coordinate of atom α, $r_{\alpha\beta} = \sqrt{(y_\alpha-y_\beta)^2+(z_\alpha-z_\beta)^2}$, L represents the distance between image planes and N the number of image charges we use for the correction (of course we can not take an infinite set of image charges as explained for the point charge between grounded planes) . We use the HOMO charge distributions to estimate the screening correction $\Delta_{occupied}$ for the occupied states and the LUMO charge distribution to obtain $\Delta_{unoccupied}$ for the unoccupied states. As we explained before, the screening correction relies on the assumption that screening by the electrodes can be described classically as two flat conductors characterized by an image plane which we can calculate using DFT (for other geometries this effect can be much more complicated). The resulting shifts within the DFT+Σ approximation are then:

$$\Sigma_{occupied} = -IP - \epsilon_H + \Delta_{occupied} \qquad \Sigma_{unoccupied} = -EA - \epsilon_L - \Delta_{unoccupied} \tag{33}$$

where the only factor that changes with respect to the previous correction is the screening. The HOMO (LUMO) is shifted up (down) with $\Delta_{occupied}$ and $\Delta_{unoccupied}$ according to their Mulliken populations and positions. To understand the differences between both methods we show an example: A Benzenedithiolate (BDT) molecule between Au leads.

2 BDT between Au leads

An archetypic example that has been extensively studied experimentally and theoretically is the BDT molecule coupled to gold contacts. In fact, it is one of the examples that GOLLUM uses to explain the image charge method. We chose (001) gold leads with nine atoms per slice, two slices on each side of the extended molecule, and three additional slices to the left and two to the right to include the bulk leads (Figure 13).

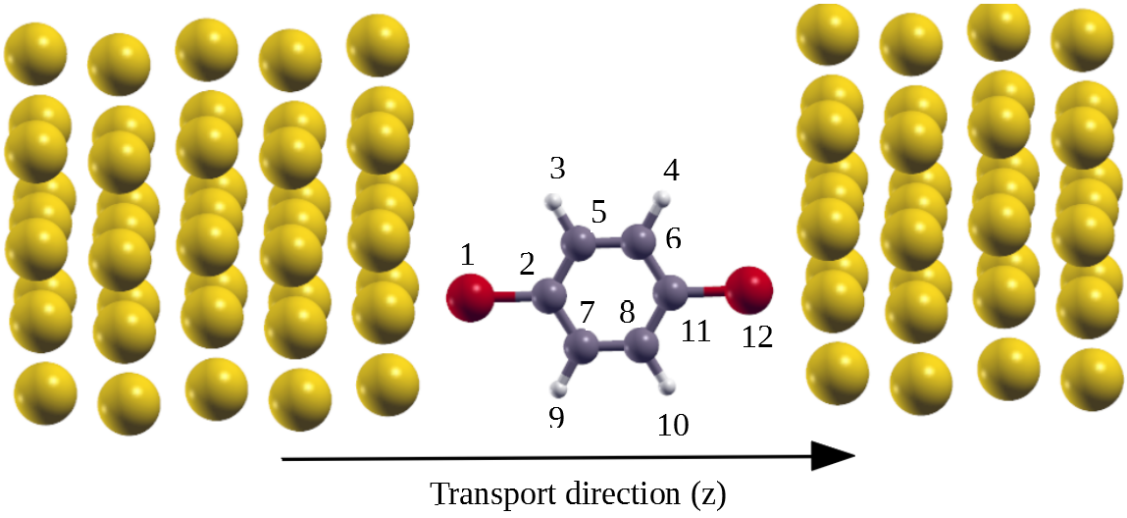

Figure 13: BDT molecule connected to (001) Au leads. Dark grey, red, white and yellow spheres are used to represent C, S, H and Au atoms respectively. Numeric labels are also included to identity each atom of the BDT molecule

We also include periodic boundary conditions along the perpendicular directions to make sure that the transmission coefficients were smooth. A SZ basis set for gold and hidrogen with s orbitals is chosen while for sulfur and carbon atoms s and p orbitals are used . This basis is too simple to understand the problem in depth or to compare to an experiment but it is enough to see the differences between the previous and the new screening correction. For the exchange and correlation functional the generalized gradient approximation is used within Perdew–Burke-Ernzerhof (PBE) parametrization. The energy cut-off is set

at 200 Ry: this cut-off defines the mesh where the jump and the overlap integrals between orbitals are solved (note that electron density is a function of position). The larger the cut-off the more accurate simulation at the cost of being computationally more demanding. Also 90 k-points are taken along the transport direction z while 1 k-point along the perpendicular directions. With all these parameters we run SIESTA and obtain the energy of the atomic levels without any of the corrections mentioned above. The implementation of the gas phase correction has not changed from the previous correction to the new one; we calculate the energy of the molecule with one electron more and one less which allows us to calculate the electron affinity and ionization potential and shift the HOMO and the LUMO accordingly. On the other hand, to apply the new screening correction we need the position of all the atoms of the molecule and their Mulliken populations; specifically of the HOMO and the LUMO that are the ones used to shift the levels up or down (Figure 14):

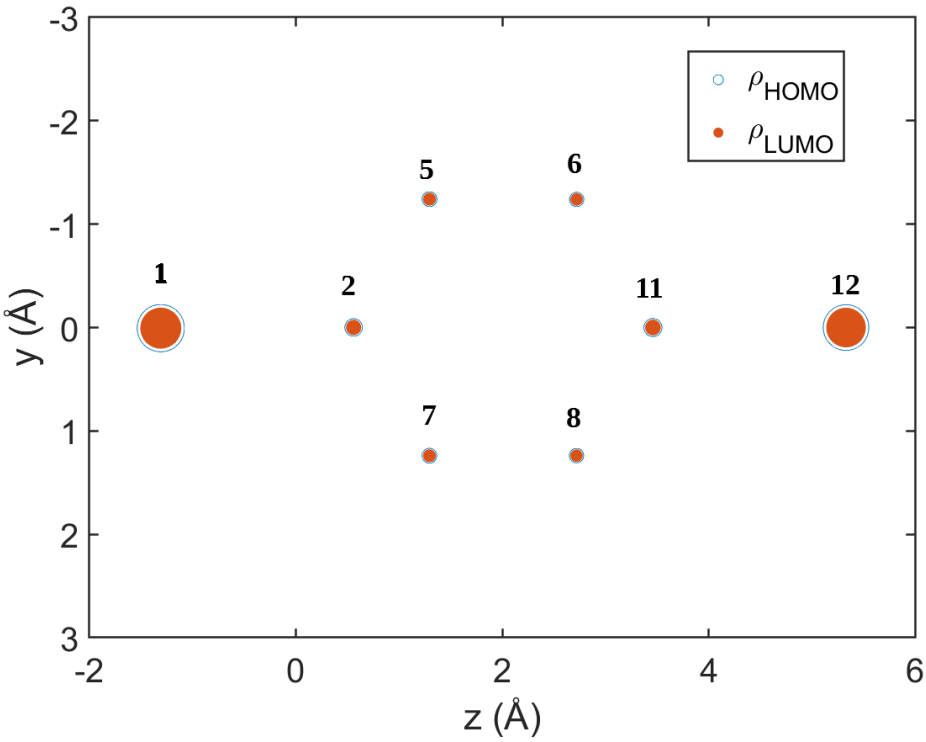

Figure 14: Scatter plot of Mulliken population of HOMO and LUMO. Only atoms with a different Mulliken population from zero are plotted.

In (Table 1) we summarize the Mulliken population of the HOMO and LUMO in units of the electron charge. In order to define the precise HOMO-LUMO gap and compare the previous and the new screening correction it is necessary to know the DFT HOMO (ϵ_H), LUMO (ϵ_L) , the IP and EA (obtained by total energy differences).

Position	$\rho_{HOMO}(q_{electron})$	$\rho_{LUMO}(q_{electron})$
1	0.3833	0.3826
2	0.0535	0.0532
5	0.0382	0.0382
6	0.0382	0.0382
7	0.0358	0.0356
8	0.0355	0.0356
11	0.0566	0.0565
12	0.3576	0.3572

Table 1: Mulliken populations of HOMO and LUMO. Only atoms with a different one from zero are shown.

The DFT HOMO, DFT LUMO, IP and EA are, respectively, -4.68, -1.38, 7.19 and -1.22 eV, from where we obtain gas phase corrections of -2.51 and 2.60 eV, for the occupied and unoccupied levels, respectively [5]. To test the previous screening correction scheme we work with two different cases (1) We assume that the image charge plane is on the surface and the point charge is in the middle of the molecule, so that $a = d/2$ where d is the distance between surfaces (a=5.34Å, arbitrary). (2) We take a as the distance between the last atom of gold of the lead and the closest sulfur atom of the molecule (a=2.05Å). This distance will make much more physical sense because as we have seen in (Figure 14) almost all the charge of the molecule is located at the sulfur atom; the weight of this interaction will contribute a lot to the total. For the new correction the image plane position can be calculated for a single flat surface using DFT yielding values of 1Å outside the last metal layer [6]. We take then the distance between the image planes as the distance between contacts L=10.7Å and this distance $\pm$1Å (Table 2)

a (Å)	$\Delta_{occupied}$ (eV)	$\Delta_{unoccupied}$ (eV)	$\Sigma_{occupied}$ (eV)	$\Sigma_{unoccupied}$ (eV)
2.05	4.6140	4.7040	2.1004	-2.0040
5.34	1.7761	1.8661	-0.7339	0.8339
L (Å)	$\Delta_{occupied}$ (eV)	$\Delta_{unoccupied}$ (eV)	$\Sigma_{unoccupied}$ (eV)	$\Sigma_{occupied}$ (eV)
9.70	0.3752	0.3069	2.2931	-2.1348
10.70	0.3646	0.3009	2.2991	-2.1454
11.70	0.3555	0.2958	2.3042	-2.1545

Table 2: HUMO and LUMO energy shifts due to screening corrections for the previous (up) and the new scheme (down)

The first striking result is that for a=2.05 Å, the distance that makes more physical sense, the shifts are done in opposite directions to the rest of the calculation (it shifts the HOMO up and the LUMO down in energy). The screening correction is larger than the gas phase correction; the interaction is being overcorrected (the charges are overscreening the interaction between the molecule and the surface). **Rigorously there is no reason for this not to happen but here it only depends on the decision of the user (arbitrary)**. It is easy to obtain an analytical expression of the distance under which this phenomena appears:

$$a < \frac{e^2}{8\pi\epsilon_0} \frac{ln(2)}{(IP + \epsilon_H)} \tag{34}$$

In fact we can see on (Table 2) that the screening correction for the occupied and unoccupied levels for a=2.05Å is huge. To show how the previous correction does not predict the physical properties correctly we plot the transmission function through the molecule for a=2.05Å, a=5.34Å (we already explained why) and a=3.05Å to compare with them (Figure 15).

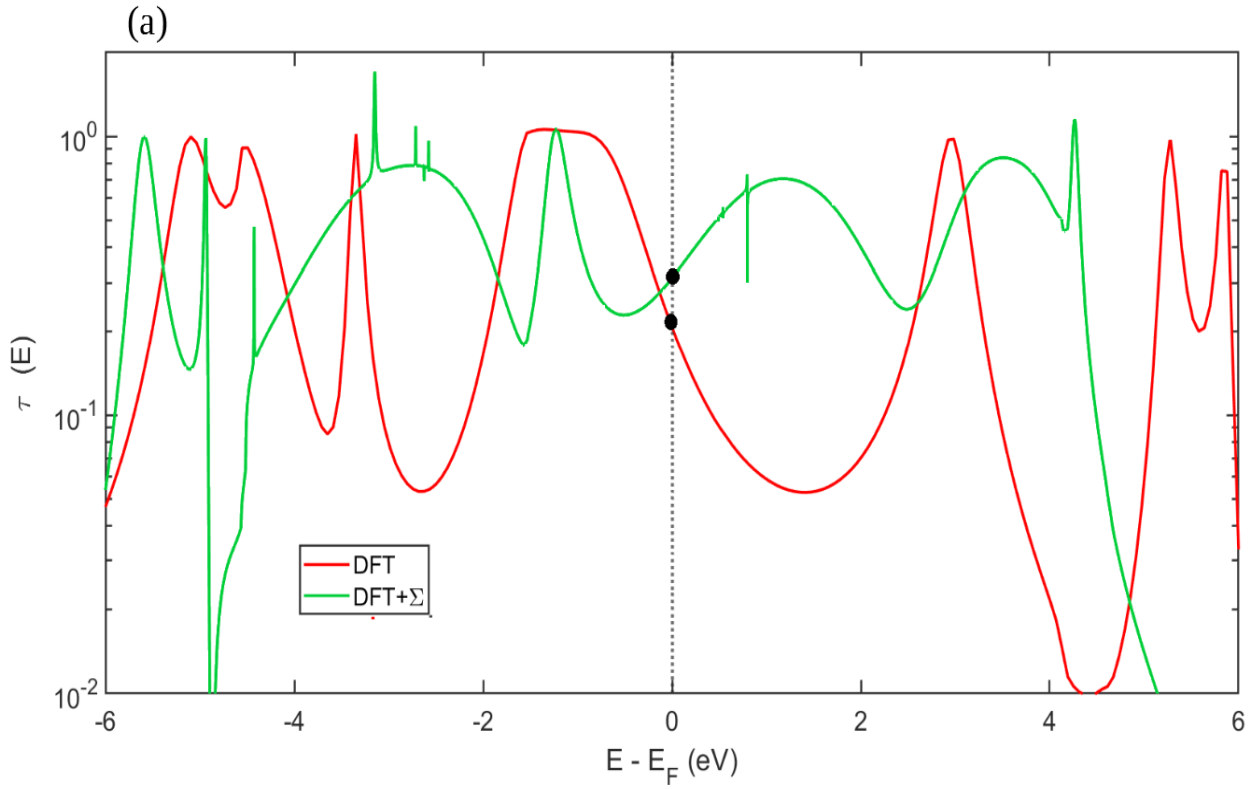
(a)
10^0
10^{-1}
10^{-2}
τ (E)
DFT
DFT+Σ
-6
-4
-2
0
2
4
6
E - E_F (eV)

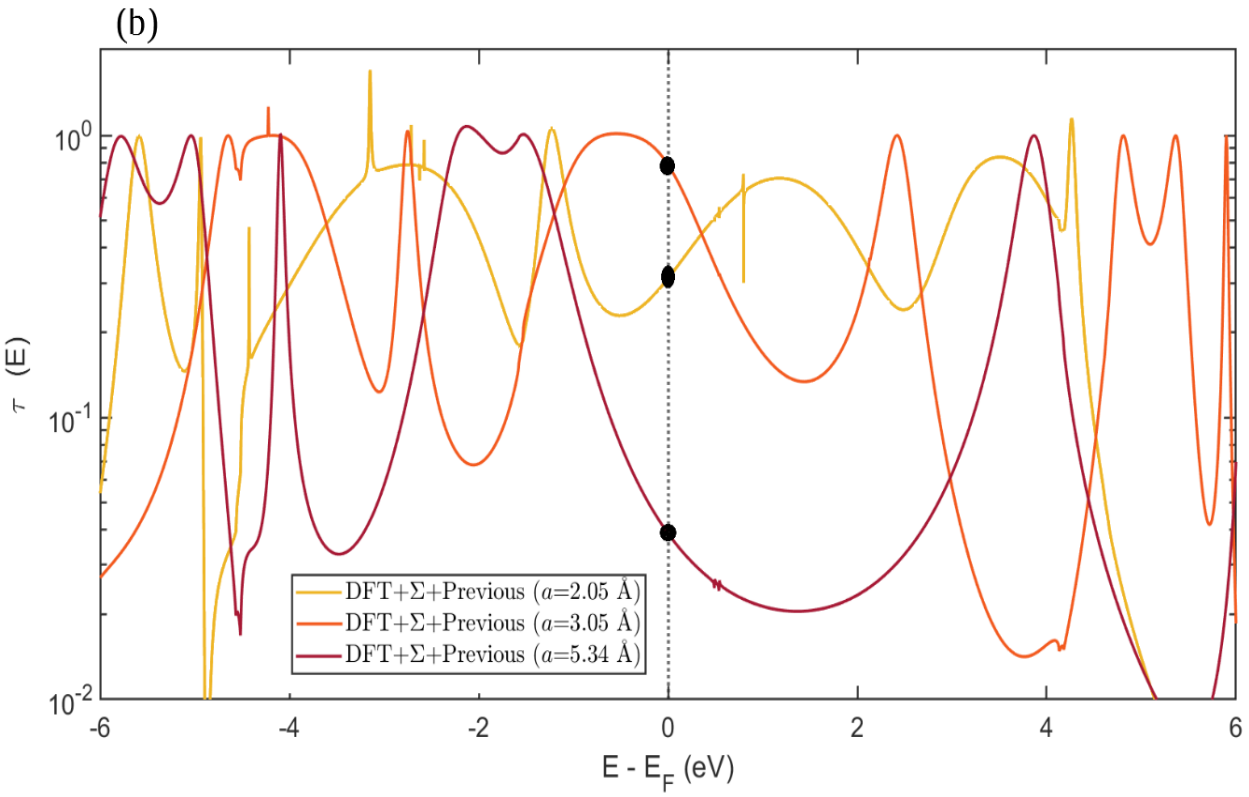
(b)
10^0
10^{-1}
10^{-2}
τ (E)
DFT+Σ+Previous (a=2.05 Å)
DFT+Σ+Previous (a=3.05 Å)
DFT+Σ+Previous (a=5.34 Å)
-6
-4
-2
0
2
4
6
E - E_F (eV)

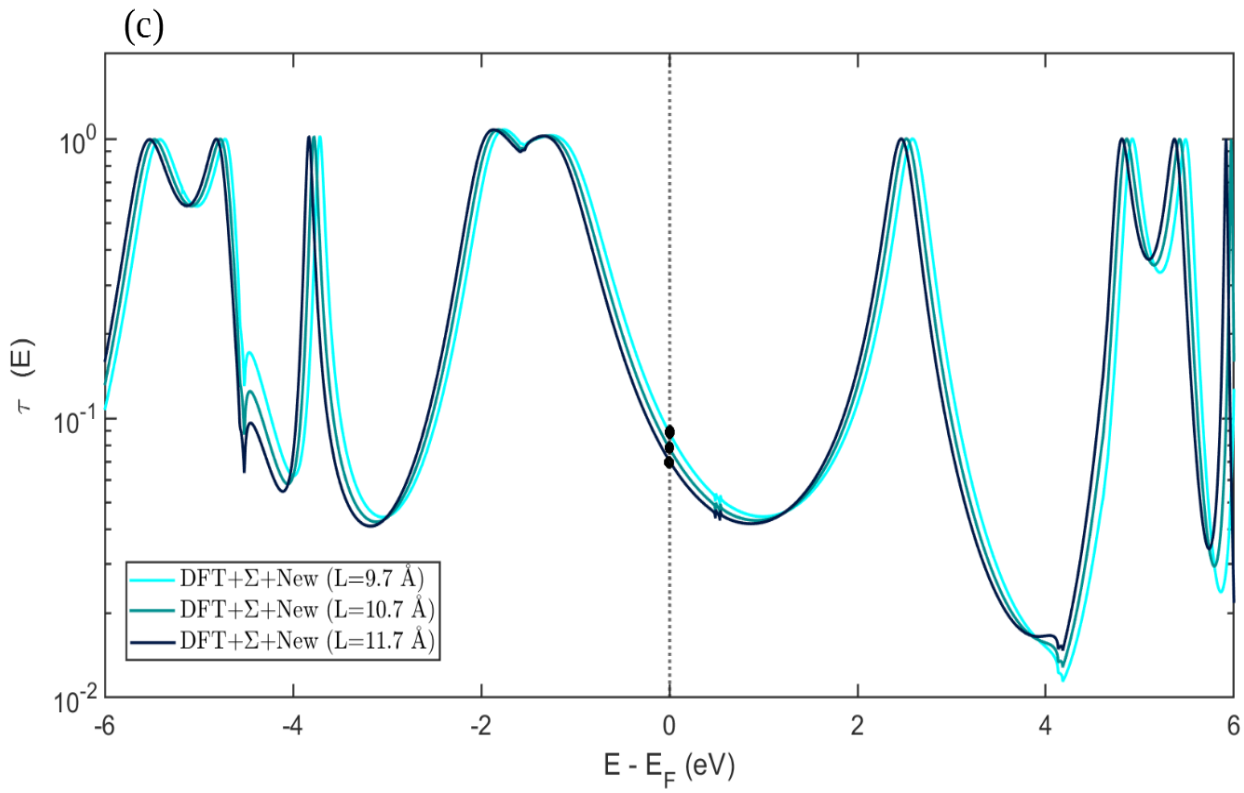

Figure 15: Transmission function for the DFT calculation on a logarithmic scale (a) Without corrections and with the gas phase correction (Σ) (b) Previous screening correction with a=2.05Å, a=3.05Å and a=5.34Å (c) New screening correction with L=9.7Å, L=10.7Å and L=11.7Å. The black points represent the conductance G obtained.

For a=2.05Å and a=3.05Å the HOMO and LUMO shifts are done in opposite directions to the expected and there is not an HOMO-LUMO gap. This does not match the prediction of the new screening correction (Figure 15). **We will only have the correct results for some values of a that in principle we don't know** (this kind of prediction is not trustworthy). For the new correction a gap appears for all the distances we choose and the HOMO-LUMO shifts are done in the direction expected. Probably at some distance our simulation will have this problem of overcorrection but it will have a physical meaning and will not depend on the choice of the user. We show the difference between the previous and the new image correction better on (Figure 16).

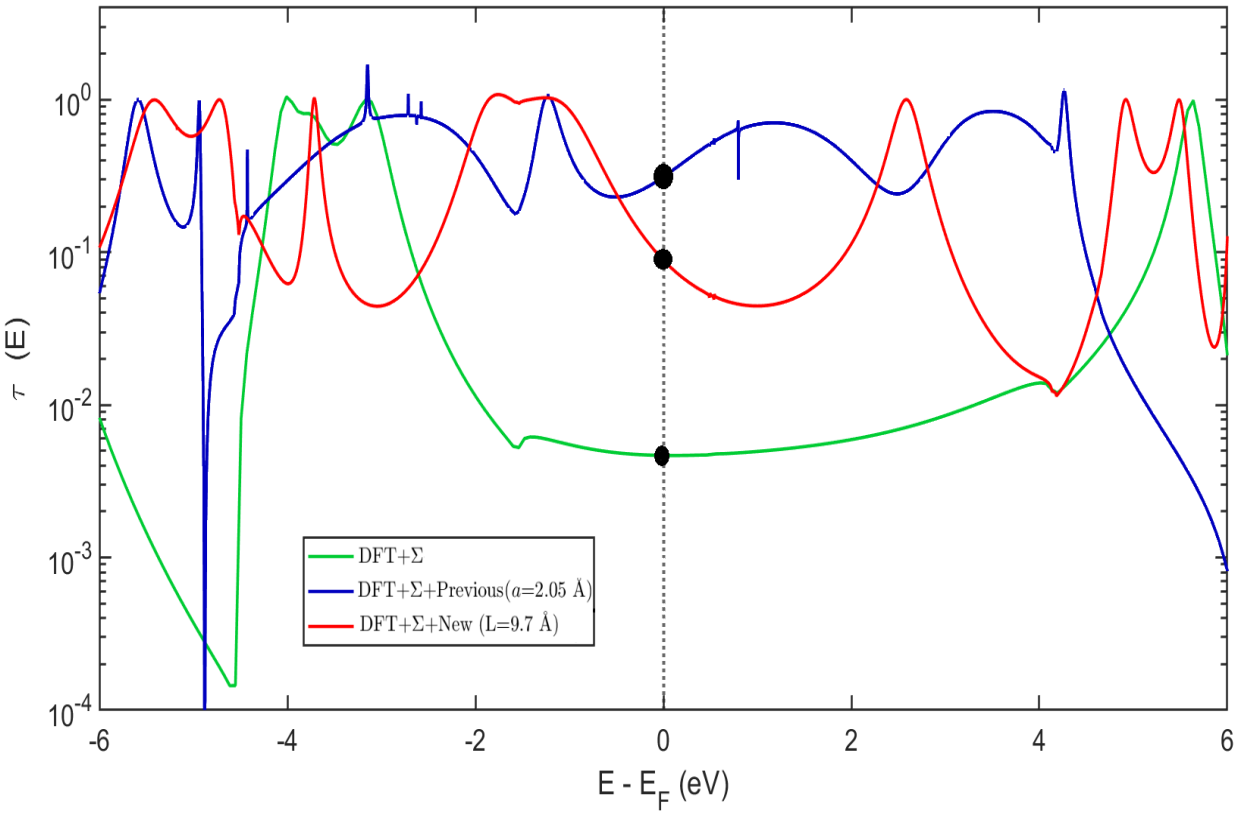

Figure 16: Transmission function for the DFT calculation on a logarithmic scale with the gas phase correction, with the previous screening correction with a=2.05Å and the new one with L=9.7Å.The black points represent the conductance G obtained.

To compare these results with experiments in the future it is interesting to show the conductance results for both methods (Table 3).

a (Å)	G (G_0)	L(Å)	G(G_0)
DFT+Σ	0.0046		
2.05	0.3254	9.7	0.0891
3.05	0.7902	10.7	0.0790
5.34	0.0380	11.7	0.0707

Table 3: Conductance calculation for the model without screening correction (DFT+Σ) and for the previous (left) and new scheme (right)

For the previous correction it may look strange the huge changes in conductance from a= 2.05Å to a= 3.05Å where it doubles and it decays in two orders of magnitude for a= 5.34Å. Again at this point we can see that **the user choice can change completely the behaviour of the simulation and the system making almost impossible to predict the results of an experiment**. To finish this thesis we show a comparison of the conductance as a function of a (where we have added some more points) and L for the previous and the new screening correction.

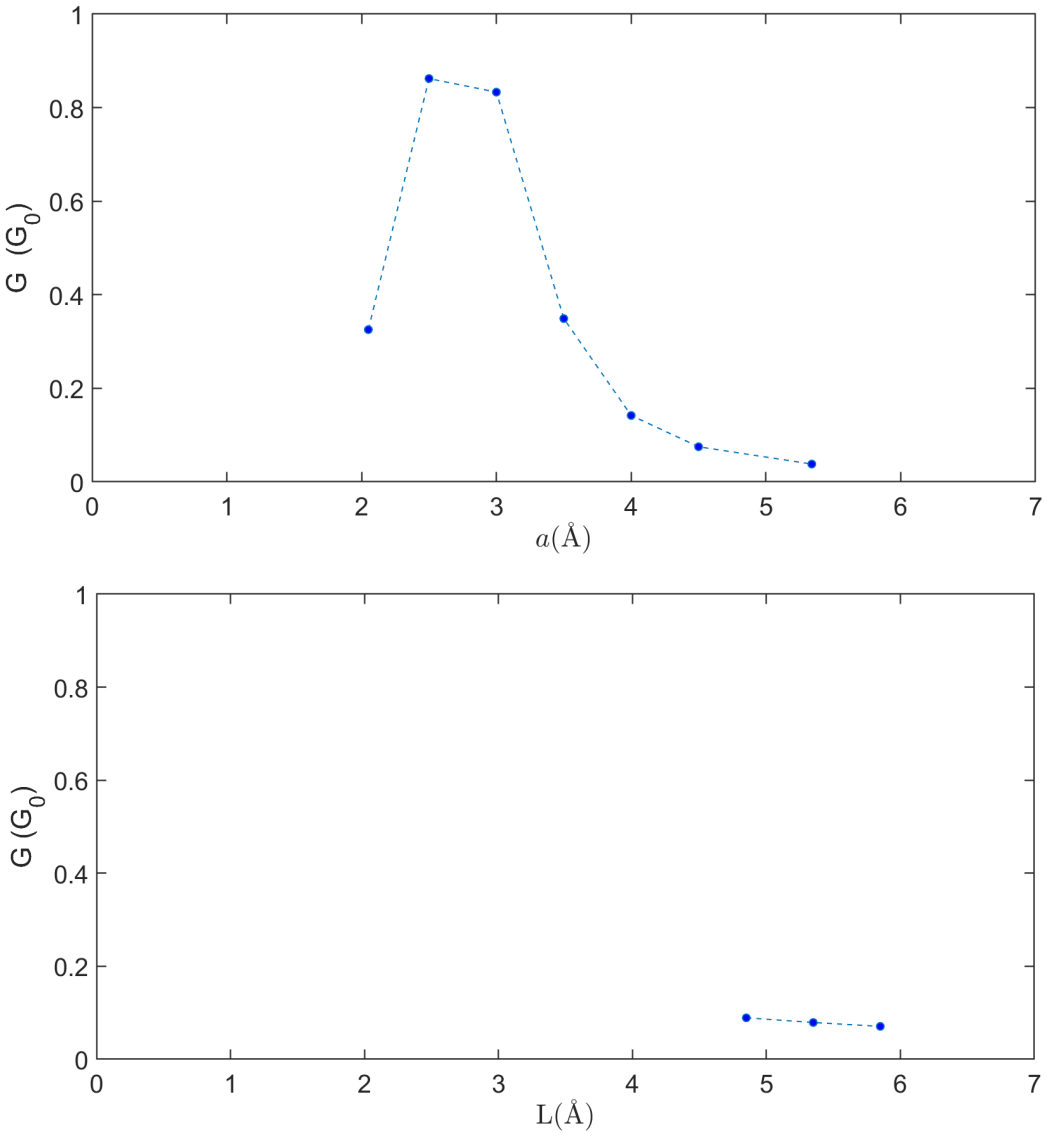

Figure 17: (Up) Conductance vs a for the previous correction (Down) Conductance vs L for the new correction where we have divided L by two

We can conclude with it that not only a is chosen arbitrarily but also that the simulation has a strong dependence on its value. On the other hand, small changes of the distance between image planes in the new correction don't affect the conductance too much (we have to remember that the possible values of L are given, we do not have the possibility to choose whatever we want). The problem of the uncertainty in L for our case is not as important as for the previous image charge correction. With these results the fundamental idea of this work ,the arbitrariness of the previous screening correction and the strong dependence of the simulation with a have been explained and shown. Our motivation from the beginning was to correct it with a model that had more physical sense and was more precise. This correction makes GOLLUM a more precise tool.

In the future we would like to test our results experimentally for a wide variety of molecules with different geometries and chemical compositions. Apart from that, the effect of applying a voltage to the planes in the screening correction will be studied. We now show the analytical results obtained during the development of these thesis even though they are not implemented in GOLLUM.

3 Charge in front of plane with potential V^*

Now that we have already seen the result for the charge in front of a grounded plane, our next question is, what will happen if we apply a potential V^* to the plane. The scheme is the same that in (Figure 10) but the boundary conditions and so the equations are different:

$$V_O = \frac{1}{4\pi\epsilon_0}\left(\frac{q}{d} + \frac{Q}{h}\right) = V^* \qquad V_P = \frac{1}{4\pi\epsilon_0}\left(\frac{q}{\sqrt{d^2+a^2}} + \frac{Q}{\sqrt{h^2+a^2}}\right) = V^* \quad (35)$$

To solve them a first idea is to take $a = d$ (it may seem possible because the potential is the same for all the points in the plane). We then get to ($\widehat{V} = 4\pi\epsilon_0 V^*$):

$$h^2 = \frac{q^2}{\left((1-\frac{1}{\sqrt{2}})\widehat{V} + \frac{q}{\sqrt{2}d}\right)^2} - d^2 \qquad Q = \left(\widehat{V} - \frac{q}{d}\right) h \tag{36}$$

Unfortunately, the result depends on the a value we choose; the problem has no exact solution. We present an alternative method for two planes with different applied potential on next section. At least this result helps us to make a physical picture of what is happening. As we change the applied potential, the image charge and its position will change, shifting the energy levels up or down tuning the conductance through the junction. We have to take into account that the image charge method is a mathematical trick and some of its results have no physical meaning (e.g. charges smaller than the one of the electron). Let's generalize this result for two plates with applied potential V_1^* and V_2^*

4 Charge between planes with V_1^* and V_2^*

The scheme is the same that in (Figure 11) but we apply a voltage V_1^* to the left electrode and V_2^* to the right. Using the results in last section we get to:

$$Q_2 = \left(\widehat{V_2} - \frac{q}{d_1}\right) d_2 \qquad Q_3 = \left(\widehat{V_1} - \frac{q}{L-d_1}\right) d_3 \tag{37}$$

The distances are then:

$$d_2^2 = \frac{q^2}{\left((1-\frac{1}{\sqrt{2}})\widehat{V_2} + \frac{q}{\sqrt{2}d_1}\right)^2} - d_1^2 \qquad d_3^2 = \frac{q^2}{\left((1-\frac{1}{\sqrt{2}})\widehat{V_1} + \frac{q}{\sqrt{2}(L-d_1)}\right)^2} - (L-d_1)^2 \tag{38}$$

With an external applied voltage we can change the value of the image charge and their positions; it will influence the interaction between the leads and the molecule shifting the levels in a different way from the ones we have explained in this thesis. As in the two grounded conducted planes once we know the distances of the first image charges we cancel their contributions by pairs (Equation 22 and 23). As we have explained in the previous section an alternative method is needed to solve this problem (because of the result dependance with a). The scheme is the same as in (Figure 11), we put a charge in the middle of the plates and we add an infinite set of image charges to cancel them by pairs. After that we add two charges, one to the right part of the right plate (Q_{right}) at a distance L_2 from it and one to the left part of the left plate (Q_{left}) at a distance L_1 to fix the voltage we want at the plates. With this method we get to:

$$\widehat{V_1} = \frac{Q_{left}}{L_1} + \frac{Q_{right}}{L_2 + L} \qquad\qquad \widehat{V_2} = \frac{Q_{right}}{L_2} + \frac{Q_{left}}{L_1 + L} \tag{39}$$

Solving these system of equation we get to:

$$Q_{left} = \frac{1}{\dfrac{1}{L_1 L_2} - \dfrac{1}{(L_2 + L)(L_1 + L)}} \left(\frac{\widehat{V_1}}{L_2} - \frac{\widehat{V_2}}{L_2 + L} \right) \tag{40}$$

$$Q_{right} = \frac{1}{\dfrac{1}{L_1 L_2} - \dfrac{1}{(L_2 + L)(L_1 + L)}} \left(-\frac{\widehat{V_1}}{L_1 + L} + \frac{\widehat{V_2}}{L_1} \right)$$

We can shift the atomic levels of the molecule by applying a different voltage to each of the planes. This will give us the possibility to tune conductance through the molecule. To conclude this thesis we show a comparison between the results obtained for the charge between two grounded planes and for the case where $V_1^* = -V_2^*$.

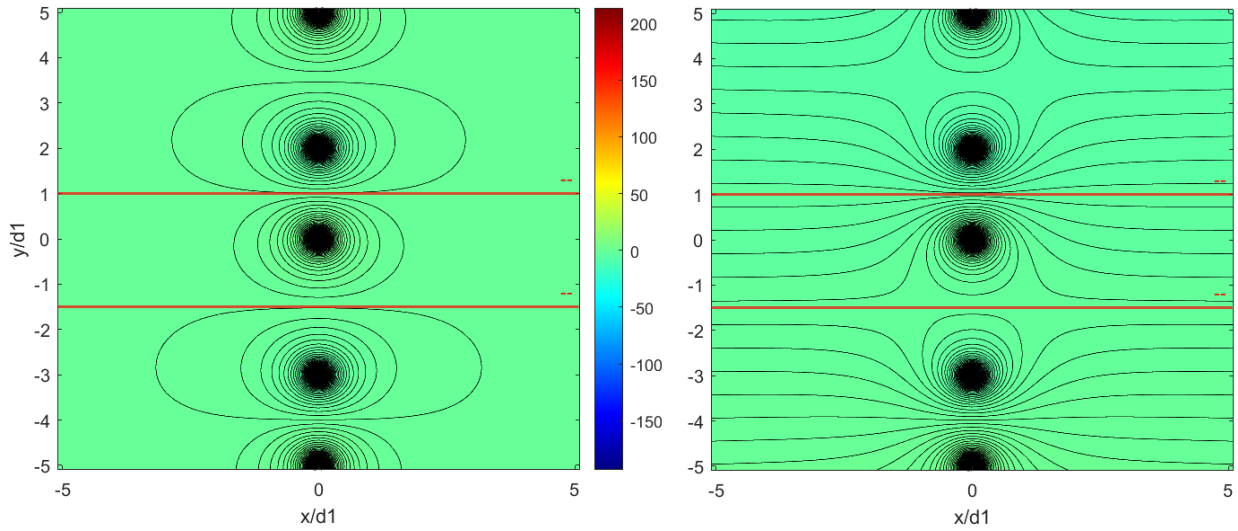

Figure 18: Equipotential surfaces for (Left) the image charge between two grounded planes (Right) the image charge between planes with $V_1^* = -V_2^*$. The red lines represent the planes.

The future image charge correction will depend of the Mulliken population of each atom and the distance to the image charge planes as it does at present but also of the potential that each of the atoms feels (it may be different for each case). Our goal in the future is to implement this case in GOLLUM to test our predictions and make it a more complete and precise simulation tool.

Summary

We have explained how DFT underestimates the HOMO-LUMO gap and how we can correct it with the gas phase and also the screening correction. To understand the first one better we work with the Hubbard dimer and how the analytical gap calculation differs from the one obtained with DFT [15]. For the second case we reviewed the simplest image charge calculations and how we can generalize them from a quantum mechanical point of view [2,4,6]. With that results we studied how to shift the position of the occupied and unoccupied molecular resonances in ab initio transport calculations of molecules between electrodes to obtain gaps and transport properties. We pointed out the fundamental problem of the previous screening correction implemented in GOLLUM; the arbitrariness. This model depended of an effective distance that has not a clear physical criteria to be chosen. In fact, when we make it match with experimental values the transmission function obtained and thus the conductance were wrong (very difficult to study molecules we do not know). An alternative method that depends only on physical parameters that we know from the beginning is proposed (atoms position and Mulliken population) [2,4,6]. With it we remove all this arbitrariness improving at least the qualitative and we hope the quantitative agreements with experiments. To test the accuracy of the method we worked with one of the most studied molecules, the BDT molecule coupled to gold leads finding that our results were more complete and precise than the previous ones. Last but no least we show our analytical results for the effect of the application of a voltage to the planes (contacts) and how it can shift the levels up or down changing the transmission function and thus the conductance. In the future we will try to implement this in GOLLUM to make a more complete and precise version of this program.

References

[1] M. Fuechsle, J. A. Miwa, S. Mahapatra, H. Ryu, S. Lee, O. Warschkow, L. Hollenberg, G. Klimeck and M. Simmons, *A single-atom transistor*, Nature Nanotechnology **7**, 242 (2012).

[2] C. W. Groth, M. Wimmer, A. Akhmerov and X. Waintal, *Kwant: a software package for quantum transport*, New Journal of Physics **16**, 063065 (2014).

[3] J. Ferrer, C. J. Lambert, V. M. García-Suárez, D. Manrique, D. Visontai, L. Oroszlany, R. Rodríguez-Ferradás, I. Grace, S. W. D. Bailey and K. Gillemot, *GOLLUM: a next-generation simulation tool for electron, thermal and spin transport*, New Journal of Physics **16**, 093029 (2014).

[4] J. M. Garcia-Lastra, C. Rostgaard, A. Rubio and K. S. Thygesen, *Polarization-induced renormalization of molecular levels at metallic and semiconducting surfaces*, Physical Review B **24**, 245427 (2009).

[5] V. M. García-Suárez and C. Lambert, *First-principles scheme for spectral adjustment in nanoscale transport*, New Journal of Physics **5**, 053026 (2011).

[6] F. Pauly, J. K. Viljas and J. C. Cuevas, *Electron-vibration interaction in transport through atomic gold wires*, Physical Review B **78**, 035315 (2008).

[7] K. S. Thygesen and A. Rubio, *Renormalization of Molecular Quasiparticle Levels at Metal-Molecule Interfaces: Trends across Binding Regimes*, Physical Review Letters **102**, 046802 (2009).

[8] J. B. Neaton, M. S. Hybertsen, and S. G. Louie, *Renormalization of Molecular Electronic Levels at Metal-Molecule Interfaces*, Physical Review Letters **97**, 216405 (2006).

[9] M. Strange and K. S. Thygesen, *Towards quantitative accuracy in first-principles transport calculations: The GW method applied to alkane/gold junctions*, Beilstein Journal of Nanotechnology **102**, 046802 (2009).

[10] S. Datta, *Quantum Transport: Atom to Transistor*, Cambridge: Cambridge University Press. (2005).

[11] T. Markussen, C. Jin and K. S. Thygesen, *Quantitatively accurate calculations of conductance and thermopower of molecular junctions*, Physica Status Solidi **11**, 2394–2402 (2013).

[12] R. P. Feynman , *The Feynman lectures on physics*, Reading Mass :Addison-Wesley Pub. Co. 1918-1988 (1963).

[13] D. J. Griffiths, *Introduction to electrodynamics*, Upper Saddle River, N. J. Prentice Hall. (1999).

[14] R. Landauer, *Spatial Variation of Currents and Fields Due to Localized Scatterers in Metallic Conduction* , IBM Journal of Research and Development **1**, 223-231 (1957).

[15] D. J. Carrascal, J Ferrer, J. C. Smith and K. Burke, *The Hubbard Dimer: A density functional case study of a many-body problem*, Journal of Physics: Condensed Matter **27**, 393001 (2015).

[16] P. Hohenberg and W. Kohn, *Inhomogeneous Electron Gas*, Physical Review **136** B864 (1964).

[17] J. F. Janak, *Proof that* $\partial E/\partial n_i = \epsilon_i$ *in density-functional theory*. Physical Review B **18** (1978) 7165.

[18] J. M. Soler, Artacho, E., Gale, J. D., García, A., Junquera, J., Ordejón, P., Sánchez-Portal, D. (2002). The SIESTA method for ab initio order-N materials simulation. Journal of Physics: Condensed Matter, 14(11), 2745.

Appendix: Mulliken population

We have a non-orthogonal basis set $|\mu\rangle$, such that $\langle\mu|\mu'\rangle = S_{\mu\mu'}$ and define the dual basis as:

$$|\mu^*\rangle = \sum_{\mu'} S^{-1}_{\mu\mu'} |\mu'\rangle \longrightarrow S^{-1}_{\mu\mu'} = \langle\mu^*|\mu'^*\rangle \tag{41}$$
$$|\mu\rangle = \sum_{\mu'} S_{\mu\mu'} |\mu'^*\rangle \longrightarrow \delta_{\mu\mu'} = \langle\mu|\mu'^*\rangle$$

We then decompose a state $|\widehat{\psi_n}\rangle$ as:

$$|\widehat{\psi_n}\rangle = \sum_{\mu} \langle\mu^*|\widehat{\psi_n}\rangle |\mu\rangle = \sum_{\mu} \widehat{C_n}(\mu) |\mu\rangle = \sum_{\mu} \begin{pmatrix} C_{n\uparrow}(\mu) \\ C_{n\downarrow}(\mu) \end{pmatrix} |\mu\rangle \tag{42}$$

To calculate the Mulliken population of an atom, first we need to know how a linear operator $\widehat{A}$ acts over the states $|\mu\rangle$:

$$\widehat{A} = \sum_{\mu\mu'} |\mu^*\rangle \langle\mu|\widehat{A}|\mu'\rangle \langle\mu'^*| = \sum_{\mu\mu'} |\mu^*\rangle A_{\mu\mu'} \langle\mu'^*| = \sum_{\mu\mu'} |\mu\rangle \langle\mu^*|\widehat{A}|\mu'^*\rangle \langle\mu'| = \sum_{\mu\mu'} |\mu\rangle \widetilde{A_{\mu\mu'}} \langle\mu'| \tag{43}$$

where we denote A=$\langle A\rangle$ and $\widetilde{A}$=$\langle\widetilde{A}\rangle$ so $A = S\widetilde{A}S$ and $\widetilde{A} = S^{-1}AS^{-1}$. With all this we compute the density operator:

$$\widehat{\rho} = \sum_{n} |\widehat{\psi_n}\rangle f_n \langle\widehat{\psi_n}| = \sum_{\mu\mu'} |\mu\rangle \sum_{n} \langle\mu^*|\widehat{\psi_n}\rangle f_n \langle\widehat{\psi_n}|\mu'^*\rangle \langle\mu'| = \sum_{\mu\mu'} |\mu\rangle \widetilde{\rho_{\mu\mu'}} \langle\mu'| \tag{44}$$

With it we can define the Mulliken population of an orbital as:

$$\widehat{N_{orbital}} = (\widetilde{\rho}S)_{\mu\mu} \tag{45}$$

And so the total atom Mulliken population is the sum to all the Mulliken population of its orbitals:

$$\widehat{N} = Tr(\rho S^{-1}) = Tr(S\widetilde{\rho}) = Tr(\widetilde{\rho}S) \tag{46}$$